

ATTACHMENT II

APPROXIMATE METHODS TO CALCULATE RADIONUCLIDE DISCHARGES FOR PERFORMANCE ASSESSMENT OF HLW REPOSITORIES IN FRACTURED ROCK

K. L. Erickson, M. S. Y. Chu, and M. D. Siegel
Sandia National Laboratories
Albuquerque, New Mexico 87185

W. Beyeler
OAO Corporation
Albuquerque, New Mexico 87108

ABSTRACT

Three approximate methods appear useful for calculating radionuclide discharges in fractured, porous rock: (1) a semi-infinite-medium approximation where radionuclide diffusion rates into the matrix are calculated assuming a semi-infinite matrix; (2) a linear-driving-force approximation where radionuclide diffusion rates into the matrix are assumed to be proportional to the difference between bulk concentrations in the fracture fluid and in the matrix pore water; and (3) an equivalent-porous-medium approximation where radionuclide diffusion rates into the matrix are calculated assuming that the time rate of change of the bulk radionuclide concentration in the matrix is proportional to the time rate of change of the radionuclide concentration in the fracture fluid. A preliminary evaluation of these approximations was made by considering transport of a single radionuclide in saturated, porous rock containing uniform, parallel fractures. It was assumed that fluid flow was one-dimensional, the nuclide existed as a single chemical species, and radioactive decay and production of the nuclide were negligible. Criteria for application of each approximation were derived in terms of fundamental physicochemical parameters. For parameter values satisfying each of the criteria, the respective errors in radionuclide discharges calculated using the approximations were examined by comparing those discharges with discharges calculated rigorously. In addition, discharges were calculated with the computer code NWFT/DVM₆ which was developed at Sandia National Laboratories for use in performance assessment calculations. Agreement among results calculated with the analytical exact solution, the analytical linear-driving-force approximation and the numerical linear-driving-force approximation was good for a variety of hydrological conditions. The applicability of each approximation to performance assessment for repositories in basalt, granite, and tuff was shown using site-specific hydrologic and geochemical parameters.

INTRODUCTION

Performance assessment requires calculating radionuclide discharges for many sets of conditions for each of several scenarios. General use of rigorous convective-diffusive transport models would be impractical for performance assessment of HLW repositories in fractured, porous rock. While such rigorous calculations are desirable for demonstrating detailed understanding of physicochemical phenomena, they would be unnecessary for risk assessment if upper bounds for radionuclide discharges could be obtained from approximate models. Three approximate methods for calculating radionuclide discharges in fractured, porous rock can be used to minimize the number of rigorous computations: (1) a semi-infinite-medium approximation where radionuclide diffusion rates into the matrix are calculated assuming a semi-infinite matrix; (2) a linear-driving-force approximation where radionuclide diffusion rates into the matrix are assumed to be proportional to the difference between bulk concentrations in the fracture fluid and in the matrix pore water; and (3) an equivalent-porous-medium approximation where radionuclide diffusion rates into the matrix are calculated assuming that the time rate of change of the bulk radionuclide concentration in the matrix is proportional to the time rate of change of the radionuclide concentration in the fracture fluid.

A preliminary evaluation of each approximation was made by considering a relatively simple system involving transport of a single radionuclide in saturated, porous rock containing uniform, parallel

fractures. It was assumed that fluid flow was one-dimensional, the nuclide existed as a single chemical species, and radioactive decay and production of the nuclide were negligible. In the discussion below, the rigorous transport equations for that system are described. Each approximation is discussed; the corresponding transport equations are given, and criteria for application of each approximation are derived in terms of fundamental physical and chemical parameters which are amenable to measurement in the laboratory or field. For parameter values satisfying each of the criteria, the respective errors in radionuclide discharges calculated using the approximations are examined by comparing those discharges with discharges calculated rigorously. The applicability of each approximation to performance assessment for repositories in basalt, granite, and tuff is discussed using site-specific hydrologic and geochemical parameters.

THEORY

Radionuclide Transport in Fractured, Porous Rock

Consider a region of saturated, porous rock containing a system of uniform, parallel fractures which divide the porous matrix into parallel flat plates (Fig. 1). Assume that: (1) fluid flow occurs only in the x-direction and is negligible in the porous matrix; (2) effects due to hydrodynamic dispersion are negligible; (3) radionuclide concentrations in the fracture fluid are uniform across the fracture cross section; (4) local chemical equilibrium exists at the fracture-matrix and pore-water-matrix inter-

faces; (5) bulk radionuclide diffusion in the pore water occurs only in the z-direction; (6) surface diffusion of nuclides in the interfacial regions between pore water and mineral phases negligibly affects transport in the porous matrix; (7) radionuclide sorption is reversible and can be represented by linear isotherms; (8) colloidal transport of nuclides is negligible; (9) radionuclides exist as a single chemical species; (10) radioactive decay and production of the nuclide of interest are negligible; and (11) diffusion coefficient is a constant. Then, the material balance for a radionuclide in the fracture fluid is

$$\frac{\partial C_f}{\partial t} + v \frac{\partial C_f}{\partial x} + m_f \frac{\partial M}{\partial t} = 0 \quad (1)$$

and in the porous matrix

$$\frac{\partial C_m}{\partial t} = D_e \frac{\partial^2 C_m}{\partial z^2} \quad (2)$$

The various terms in Eqs. (1) and (2) are defined in Table I. Appropriate initial and boundary conditions for Eq. (1) are $C_f(x,0) = 0$, $M(x,0) = 0$, and $C_f(0,t) = C_0 = \text{a constant}$. Appropriate conditions for Eq. (2) are $C_m(x,z,0) = 0$, $C_m(x,B,t) = C_f(x,t)$, and $\partial C_m(x,0,t)/\partial z = 0$. The solution to Eqs. (1) and (2) is obtained analogously to Rosen's¹ results for packed beds of spheres. The fracture fluid concentration $C_f(x,t)$ is given by

$$\frac{C_f(x,t)}{C_0} = \frac{1}{2} + \frac{2}{\pi} \int_0^{\infty} e^{-\bar{x}H_{D_1}(B)} \sin\left[\bar{y}B^2 - \bar{x}H_{D_2}(B)\right] \frac{dB}{B} \quad (3)$$

where

$$\bar{x} = \frac{D_e \phi_m R_m m_f x}{vB^2} = \left(\frac{D_e}{\alpha}\right) \phi_m m_f x$$

$$\bar{y} = \frac{2D_e(t - \frac{x}{v})}{B^2}$$

$$H_{D_1}(B) = \frac{B[\sinh(2B) - \sin(2B)]}{\cosh(2B) + \cos(2B)}$$

$$H_{D_2}(B) = \frac{B[\sinh(2B) + \sin(2B)]}{\cosh(2B) + \cos(2B)}$$

$B = \text{variable of integration.}$

The integral in Eq. (3) must be evaluated numerically. However, for large \bar{x} , say $\bar{x} \geq 50$, $C_f(x,t)$ can be approximated by:

$$\frac{C_f(x,t)}{C_0} = \frac{1}{2} \left\{ 1 + \operatorname{erfc} \left[\frac{\frac{\bar{y}}{2\bar{x}} - 1}{2\sqrt{\frac{1}{3\bar{x}}}} \right] \right\} \quad (4)$$

Eq. (4) is obtained from Eq. (3) using the identity²

$$\int_0^{\infty} e^{-B^2} \sin(2\mu B) \frac{dB}{B} = \frac{\pi}{2} \operatorname{erf}(\mu)$$

and noting that $H_{D_1} \rightarrow (4/3)B^4$ and $H_{D_2} \rightarrow 2B^2$ as $B \rightarrow 0$.

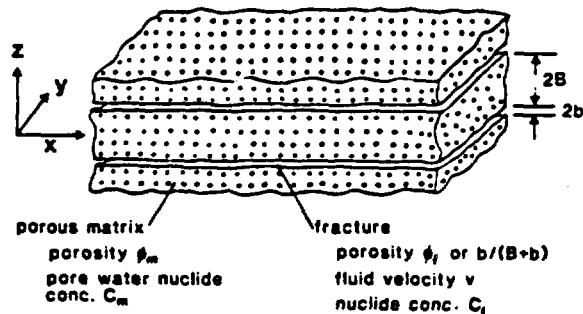


Fig. 1. Schematic representation of fractured, porous rock. Origin of coordinate system is at center of block of porous rock.

Approximations

General. The rigorous solution to Eqs. (1) and (2) can be obtained using Duhamel's theorem to express the term $M(x,t)$ in Eq. (1) as

$$M(x,t) = \frac{\phi_m R_m}{B} \int_0^B \int_0^t C_f(x,t') \frac{\partial H(z,t-t')}{\partial t} dt' dz \quad (5)$$

where $H(z,t)$ is the solution to Eq. (2) when the surface boundary condition is replaced by $C_m(x,B,t) = 1$. In each of the three approximations, a simpler expression for $M(x,t)$, or $\partial M(x,t)/\partial t$, is substituted for Eq. (5), so that the resulting solution for $C_f(x,t)$ is much simpler to obtain than Eq. (3). For convenience below, let $\bar{H}(t)$ denote the volume-averaged nuclide concentration in pore water when surface concentration is unity (see Table I), and write Eq. (5) as

$$M(x,t) = \phi_m R_m \int_0^t C_f(x,t') \frac{\partial \bar{H}(t-t')}{\partial t} dt' \quad (6)$$

Semi Infinite Medium. In this approximation, the basic assumption is that the porous matrix is so large that the concentration $C_m(x,0,t)$ of the diffusing nuclides can be considered negligible during the time interval of interest. The term $\partial H/\partial t$ in Eq. (6) is then obtained from the solution to the diffusion equation for semi-infinite, flat plates having unit surface concentration. For fluid flowing between parallel plates separated by aperture $2b$, the expression for $C_f(x,t)$ is given by³

$$\frac{C_f(x,t)}{C_0} = \operatorname{erfc} \left(\frac{\phi_m R_m x \sqrt{D_e}}{2bv \sqrt{t - \frac{x}{v}}} \right) = \operatorname{erfc} \left(\frac{\sqrt{2}}{2} \sqrt{\frac{\bar{x}}{\bar{y}}} \right) \quad (7)$$

Table I
Nomenclature

Term	Definition
B	half thickness of matrix between fractures
\bar{B}	B+b, half spacing between fractures
b	half of the fracture aperture
C_f	radionuclide concentration in the fracture fluid
C_m	radionuclide concentration in the matrix pore water
D	molecular diffusion coefficient for the radionuclide in the matrix pore water
D_e	$D/\alpha^2 R_m$
$H(z,t)$	solution to Eq. 2 when the surface boundary condition is replaced by $C_m(x,B,t) = 1$
$\bar{H}(t)$	$\frac{1}{B} \int_0^B H(z,t) dz$, the volume average of $H(z,t)$
ϕ_f	b/\bar{B} , porosity associated with the fractures
ϕ_m	matrix porosity
m_f	$(1-\phi_f)/\phi_f$
m_m	$(1-\phi_m)/\phi_m$
M	$\phi_m R_m \left(\frac{1}{B}\right) \int_0^B C_m dz$, the average matrix radionuclide concentration
R_m	$(1+m_m \Gamma_0)$, radionuclide retardation factor for the porous matrix
t	time
v	mass-averaged fracture fluid velocity
x	spatial coordinate in the direction of the bulk fluid motion
z	spatial coordinate in the direction of diffusion in the porous matrix
α^2	tortuosity/constrictivity factor for the porous matrix
Γ_0	slope of the linear portion of the dimensionless sorption isotherm (fluid- and solid-phase concentrations both expressed as mass or moles per unit volume)
\bar{x}	$\frac{D m_f \phi_m x}{\alpha^2 v B^2}$
\bar{y}	$\frac{2D_e (t-x/v)}{B^2}$

The relative errors in C_f which result from using Eq. (7) rather than Eq. (3) are determined by the corresponding errors in the value for $M(x,t)$, which in turn depend on the errors in the value of $\partial \bar{H}/\partial t$. Criteria for using Eq. (7) can be developed as follows. First, consider one-dimensional diffusion into semi-infinite flat plates such as depicted in Fig. 1. Let $z' = B - z$, and $C_m(z' = 0, t) = 1$. The corresponding expressions for $\bar{H}(z', t)$ and $\bar{H}(t)$ are given, respectively, by⁴

$$\bar{H}(z', t) = \operatorname{erfc}\left(\frac{z'}{2\sqrt{D_e t}}\right) \quad (8)$$

and

$$\bar{H}(t) = \frac{2}{\sqrt{\pi}} \left(\frac{D_e t}{B^2}\right)^{1/2} \quad (9)$$

As the time interval of interest increases, the value of $\bar{H}(t)$ determined from Eq. (9) will be increasingly in error, as can be seen by inspection of the expression from the exact solution⁵ for "short times"

$$\bar{H}(t) = 2 \left(\frac{D_e t}{B^2}\right)^{1/2} \left\{ \frac{1}{\sqrt{\pi}} + 2 \sum_{n=1}^{\infty} (-1)^n \operatorname{erfc}\left(\frac{nB}{\sqrt{D_e t}}\right) \right\} \quad (10)$$

Let \bar{H}_a and \bar{H}_e denote the values of \bar{H} obtained from Eqs. (9) and (10), respectively, and let $F_a = (\partial \bar{H}_a/\partial t)/(\partial \bar{H}_e/\partial t)$. Eq. (6) then can be written as

$$M(x,t) = \phi_m R_m \int_0^t C_f(x,t') \left[\frac{1}{F_a(t-t')} \right] \frac{\partial \bar{H}_a(t-t')}{\partial t} dt' \quad (11a)$$

and by the mean value theorem⁶

$$M(x,t) = \frac{\phi_m R_m}{F_a(t-\eta)} \int_0^t C_f(x,t') \frac{\partial \bar{H}_a(t-t')}{\partial t} dt' \quad (11b)$$

where $0 \leq \eta \leq t$. The term $F_a(t-\eta) = F_a^*$ represents some mean value of $F_a(t-t')$. By definition $F_a \geq 1$.

When $F_a = 1$,

$$M(x,t) = \phi_m R_m \int_0^t C_f(x,t') \frac{\partial \bar{H}_a(t-t')}{\partial t} dt' \quad (12)$$

and when $F_a > 1$, the ratio of approximate to exact values of $M(x,t)$ is given by F_a^* . Since \bar{H}_a , \bar{H}_e , $\partial \bar{H}_a/\partial t$, $\partial \bar{H}_e/\partial t$, and F_a are single-valued functions of t , a one-to-one relationship exists between F_a and \bar{H}_e . Values of F_a as a function of \bar{H}_e are shown in

Fig. 2. For $\bar{H}_e < 0.5$, $F_a = 1$, while for $\bar{H}_e > 0.5$, F_a increases monotonically and becomes large for $\bar{H}_e > 0.8$. The value of F_a^* will be between zero and the value of $F_a(\bar{H}_e)$ corresponding to time t . For purposes here, it appears reasonable to estimate F_a^* by the average \bar{F}_a of F_a with respect to \bar{H}_e , that is

$$F_a^*(\bar{H}_e) = \bar{F}_a(\bar{H}_e) = \frac{1}{\bar{H}_e} \int_0^{\bar{H}_e} F_a(\bar{H}) d\bar{H} \quad (13)$$

Values of \bar{F}_a also are shown in Fig. 2. When $\bar{H}_e \leq 0.5$, the values of both \bar{F}_a and F_a are about 1.0. When $0.5 < \bar{H}_e \leq 0.7$, the value of \bar{F}_a is about 1.0, and F_a is 1.2 or less. When $0.7 < \bar{H}_e \leq 0.92$, the value of \bar{F}_a is between about 1.0 and 1.2, and F_a is between 1.2 and 2.8. When $\bar{H}_e > 0.92$, \bar{F}_a and especially F_a become large. Therefore, when $\bar{H}_e \leq 0.5$, the ratio of approximate to exact values of $M(x,t)$ from Eqs. (12) and (6), respectively, would be about 1.0. When $0.5 < \bar{H}_e \leq 0.7$, the ratio would be about 1.0 and would not be greater than 1.2. When $0.7 < \bar{H}_e \leq 0.92$, the ratio would be about 1.2 or less and would not be greater than 2.8.

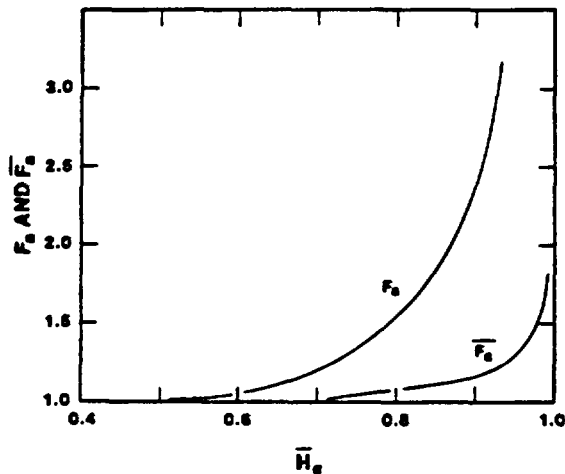


Fig. 2. Values of F_a and \bar{F}_a versus \bar{H}_e .

Criteria for applying the semi-infinite-medium approximation, that is, calculating $M(x,t)$ from Eqs. (12) and (9) rather than Eqs. (6) and (10), will depend on the errors which are acceptable in $M(x,t)$ and in calculated radionuclide discharges. When solving Eq. (1) with either approximate or exact expressions for $M(x,t)$, those expressions actually appear as $M(x,t - x/v)$, since $C_f(x,t) = 0$ if $t < x/v$ and only convective transport occurs in the x -direction in the fractures. To examine errors between approximate and exact solutions, the value for \bar{H} should correspond to the contact time $t^* = t - x/v$ rather than the elapsed time t . Conditions under which the semi-infinite-medium approximation are useful could be defined in terms of t^* . However, the use of maximum mean radionuclide contact time would lead to criteria which are more restrictive and conservative.

Let θ_m denote the maximum mean radionuclide residence time along the flow path of interest. In which case, θ_m corresponds to the fracture fluid and pore water being in equilibrium with respect to radionuclide diffusion. As discussed later, θ_m is given by $\theta_m = (x/v)R_f$, where x corresponds to the

flow path length, and R_f is the radionuclide retardation factor for the fracture fluid and is given by $R_f = 1 + \rho_f \phi_m R_m$. By analogy with t^* , define the contact residence time θ_m^* as $\theta_m - x/v$.

First, consider cases where $t^* < \theta_m^*$. From Table II, $\bar{H}_e \leq 0.5$ when $D_e t^*/B^2 \leq 0.2$, $\bar{H}_e \leq 0.7$ when $D_e t^*/B^2 \leq 0.4$, and $\bar{H}_e \leq 0.92$ when $D_e t^*/B^2 \leq 1.0$. If $\theta_m \leq 0.2B^2/D_e$, then $\theta_m^* \leq 0.2B^2/D_e$ for all x , and perturbations in radionuclide concentrations would be exposed to an essentially semi-infinite porous matrix for which $F_a = 1.0 = \bar{F}_a$ throughout. Radionuclide discharges then could be obtained from Eq. (7). If $0.2 < \theta_m(B^2/D_e) \leq 0.4$, perturbations in radionuclide concentrations would be exposed to a porous matrix for which $F_a \leq 1.2$ and $\bar{F}_a = 1.0$. Again, radionuclide discharges could be obtained from Eq. (7); however, as t and θ_m approach $0.4B^2/D_e$, small relative errors in $M(x,t)$ and, therefore, in values of C_f/C_0 should be expected since F_a will be greater than 1.0 for some values of x . If $0.4 \leq \theta_m(B^2/D_e) \leq 1.0$, perturbations in radionuclide concentrations would be exposed to a porous matrix for which $F_a \leq 2.8$ and $\bar{F}_a \leq 1.2$. The relative errors in radionuclide discharges obtained from Eq. (7) would correspond to relative errors in the value of $M(x,t)$ which are of the order of 20 percent as t and θ_m approach $1.0B^2/D_e$.

Table II
Values of $\bar{H}_e(t)$ Versus $D_e t/B^2$

$D_e t/B^2$	$\bar{H}_e(t)$	$D_e t/B^2$	$\bar{H}_e(t)$
0.0001	0.01	0.09	0.34
0.001	0.04	0.10	0.36
0.003	0.06	0.20	0.50
0.005	0.08	0.30	0.61
0.008	0.10	0.40	0.70
0.01	0.11	0.50	0.76
0.02	0.16	0.60	0.81
0.03	0.20	0.70	0.86
0.04	0.23	0.80	0.89
0.05	0.25	0.90	0.91
0.06	0.28	1.00	0.93
0.07	0.30	1.50	0.98
0.08	0.32	2.00	0.99

Next, consider cases where $t^* > \theta_m^*$. For a given ratio of $\theta_m/(B^2/D_e)$, values of \bar{F}_a will be larger than when $t^* < \theta_m^*$. Relative errors in $M(x,t)$, and the corresponding errors in radionuclide discharges, also should be larger. However, the radionuclide flux, $-D_e \partial H(0,t)/\partial z'$, is proportional to $1/t$, which follows from Eq. (8). Therefore, while the relative error associated with the semi-infinite-medium approximation increases, the relative amount of the radionuclide diffusing into the porous matrix decreases, thereby reducing the overall effect that those errors have on radionuclide discharges. In examples given later, it is shown that when $t^* > \theta_m^*$, the relative errors in radionuclide discharges do not increase appreciably beyond those corresponding to $t^* = \theta_m^*$.

If only small relative errors in calculated radionuclide discharges are acceptable, the criterion for applying the semi-infinite medium approximation is $\theta_m = (x/v)R_f \leq 0.2B^2/D_e$ or,

$$\frac{D_e R_f x}{vB^2} \leq 0.2$$

Often, $\phi_f \ll 1$, and $\phi_m > \phi_f$. Under those conditions, $R_f = m_f \phi_m R_m$ since $R_m \geq 1$. Then, the criterion for applying the approximation can be written as

$$\bar{x} = \frac{D_e m_f \phi_m R_m x}{vB^2} = \left(\frac{D_e}{v}\right) m_f \phi_m x \leq 0.2 \quad (14a)$$

when only small relative errors are acceptable.

However, it seems reasonable to define a less restrictive criterion. Parameter values in the expression for $M(x,t)$ may often involve uncertainties of 20 to 30 percent or greater, which result from inherent variations in the physical and chemical properties of geomedia. If the criterion $\theta_m = (x/v)R_f \leq B^2/D_e$ is used, relative errors in $M(x,t)$ would be on the order of 20 percent for $t \leq \theta_m$, and are similar to, or less than, possible uncertainties in parameter values. Hence

$$\bar{x} = \frac{D_e m_f \phi_m R_m x}{vB^2} = \left(\frac{D_e}{v}\right) m_f \phi_m x \leq 1 \quad (14b)$$

when relative errors of about 20 percent in $M(x,t)$ and the corresponding errors in calculated discharges are acceptable.

Linear Driving Force. In the usual form of this approximation, the radionuclide flux into the porous matrix is assumed to be proportional to the difference between the surface and average matrix concentrations, and the approximation expressed as

$$\frac{dM}{dt} = k a_m (\phi_m R_m C_f - M) \quad (15)$$

where a_m is the surface area of the porous matrix contacting the fracture fluid per unit volume of matrix, and k is a constant mass transfer coefficient which is evaluated analytically below. When Eqs. (1) and (15) are solved, the resulting expression for $C_f(x,t)$ is

$$\frac{C_f(x,t)}{C_0} = J(n,m) = 1 - e^{-m} \int_0^n e^{-B} I_0(2\sqrt{B}) dB \quad (16)$$

where $a_m = \frac{1}{B}$

$$m = \frac{k}{B} \left(t - \frac{x}{v} \right)$$

$$n = \frac{k \phi_m R_m x}{Bv}$$

and B is again a variable of integration.⁷ Values of the function $J(n,m)$ have been tabulated extensively,

and for $nm > 3600$ the function is given approximately by

$$J(n,m) = \frac{1}{2} \operatorname{erfc}(\sqrt{n} - \sqrt{m}) \quad (17)$$

In these analyses, the term $a\bar{H}/at$ in Eq. (6) was approximated using a linear-driving-force expression for diffusion into flat plates having unit surface concentration, that is

$$\frac{d\bar{H}}{dt} = k a_m (1 - \bar{H}) \quad (18)$$

For $\bar{H}(0) = 0$,

$$\bar{H} = 1 - \exp(-k a_m t) \quad (19)$$

and

$$\frac{d\bar{H}}{dt} = k a_m \exp(-k a_m t) \quad (20)$$

Substituting Eq. (20) into Eq. (6) gives

$$M(x,t) = \phi_m R_m \int_0^t C_f(x,t') \{k a_m \exp[-k a_m (t - t')]\} dt' \quad (21)$$

and it can be verified by differentiation that Eq. (21) satisfies Eq. (15) when $M(x,0) = 0$, so that the solution for $C_f(x,t)$ from Eqs. (1) and (21) is given by Eqs. (16) and (17).

To evaluate the mass transfer coefficient k , substitute for $\bar{H}(t)$ the "long-time" infinite series solution⁵ given by

$$\bar{H}(t) = 1 - \sum_{n=0}^{\infty} \frac{8}{(2n+1)^2 \pi^2} \exp\left[\frac{-D_e (2n+1)^2 \pi^2 t}{4B^2}\right] \quad (22)$$

The resulting expression for $M(x,t)$ is

$$M(x,t) = \phi_m R_m \int_0^t C_f(x,t') \left\{ \frac{2D_e}{B^2} \sum_{n=0}^{\infty} \exp\left[\frac{-D_e (2n+1)^2 \pi^2 t'}{4B^2}\right] \right\} dt' \quad (23)$$

Now, let $k = 2\gamma D_e/B$, where γ is a numerical constant, and note that $a_m = 1/B$. Comparing Eqs. (21) and (23), it can be seen that for an appropriate value of γ , on the order of 1 to $\pi^2/6$, Eq. (21) should provide a reasonable approximation for Eq. (23) when $D_e t/B^2$ is large enough so that the series in Eq. (23) can be truncated after the first term. A value for the constant γ can be obtained as follows.

Let \bar{H}_b and \bar{H}_e denote the values of \bar{H} obtained from Eqs. (19) and (22), respectively; let

$$F_b = \frac{\frac{\partial \bar{H}_b}{\partial t}}{\frac{\partial \bar{H}_e}{\partial t}} ;$$

and again apply the mean value theorem to Eq. (6). The ratio of approximate to exact values of $M(x,t)$ from Eqs. (21) and (23), respectively, is given by the term F_b^* defined analogously to F_a^* above. For very small $D_e t^*/B^2$, corresponding to small \bar{H}_e , $F_b = 0$. As $D_e t^*/B^2$ increases, and \bar{H}_e approaches unity, F_b will increase to some finite value which depends on the constant γ .

For a given value of γ , it appears reasonable to estimate F_b^* by the average F_b of F_b with respect to \bar{H}_e , that is

$$F_b = \frac{1}{\bar{H}_e} \int_0^{\bar{H}_e} F_b(\bar{H}) d\bar{H} .$$

Values of F_b as a function of \bar{H}_e are shown on Fig. 3 for $\gamma = 1.0, 1.25, 1.50,$ and 2.0 . Since the values of F_b corresponding to $\gamma = 1.5$ show the least average relative deviation about 1.0, the value for γ was taken as 1.5, from which $k = 2\gamma D_e/B = 3D_e/B$.

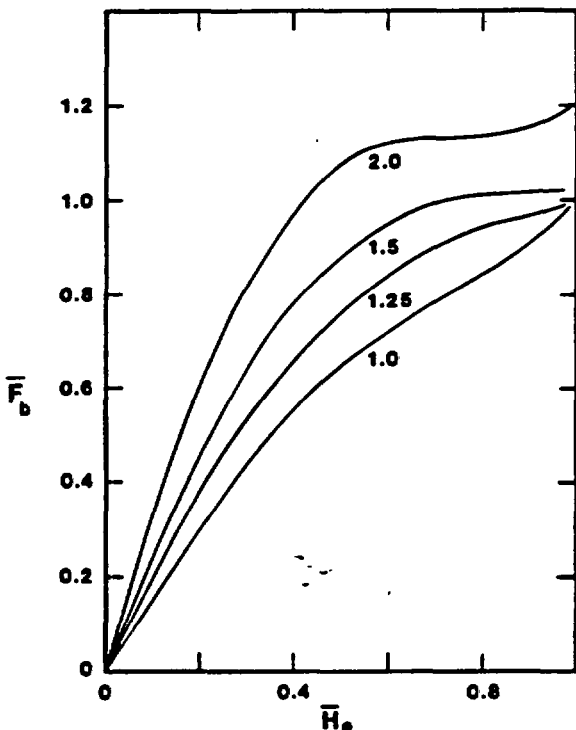


Fig. 3. Values of F_b versus \bar{H}_e (numbers on curves are values for numerical constant γ).

Criteria for applying the linear-driving-force approximation, that is calculating $M(x,t)$ from Eq. (21) with $k = 3D_e/B$, will depend on the errors which are acceptable in $M(x,t)$. To define those

criteria, it is initially assumed, and later verified, that when the linear-driving-force approximation applies, the mean radionuclide residence time is given approximately by the maximum mean residence time θ_m^* defined above. Again, let $t^* = t - x/v$ and $\theta_m^* = \theta_m - x/v$. First, consider cases where $t^* > \theta_m^*$. From Fig. 3 ($\gamma = 1.5$), $F_b = 1.0$ when $\bar{H}_e \geq 0.7$ or $D_e t^*/B^2 \geq 0.5$ (Table II). If radionuclide residence times do not vary greatly about θ_m , and if $\theta_m^* \geq 0.5B^2/D_e$, perturbations in radionuclide concentrations would be exposed to a porous matrix throughout which $F_b = 1.0$. For some cases, radionuclide residence times will vary significantly about the mean. If only small errors in radionuclide discharges are acceptable, a more conservative criterion is $\theta_m^* \geq B^2/D_e$ or

$$\bar{x} = \frac{D_e m_f \phi_m R_m x}{v B^2} = \frac{\frac{D_e}{2} m_f \phi_m x}{v B^2} \geq 1 . \quad (24a)$$

It seems reasonable to also define a less restrictive criterion since, as mentioned previously, parameter values in the expression for $M(x,t)$ may often involve uncertainties of 20 to 30 percent. From Fig. 3, $F_b \geq 0.7$ when $\bar{H}_e \geq 0.36$ or $D_e t^*/B^2 \geq 0.1$ (Table II). Therefore, if $\theta_m^* \geq 0.1B^2/D_e$, perturbations in radionuclide concentrations would be exposed to a porous matrix throughout which $0.7 \leq F_b \leq 1.0$. The relative errors in $M(x,t)$ would be similar to or less than uncertainties in parameter values. Again, allowing for variations in radionuclide residence times about θ_m , a reasonable criterion would be $\theta_m^* \geq 0.2B^2/D_e$ or

$$\bar{x} = \frac{D_e m_f \phi_m R_m x}{v B^2} = \frac{\frac{D_e}{2} m_f \phi_m x}{v B^2} \geq 0.2 . \quad (24b)$$

when errors of 20 to 30 percent in $M(x,t)$ and the corresponding errors in C_f/C_0 are acceptable.

Now consider cases where $t^* < \theta_m^*$. For a given ratio $D_e \theta_m^*/B^2$, the values of F_b will decrease as $D_e t^*/B^2$ becomes less than 0.5, while the relative errors in $M(x,t)$ and the corresponding errors in $C_f(x,t)/C_0$ will increase. If $D_e \theta_m^*/B^2$ is large, those errors will occur when $C_f/C_0 \approx 0$, since for a reasonable variation in radionuclide residence times about θ_m , C_f/C_0 will be negligible when $t^* \ll \theta_m^*$. If $D_e \theta_m^*/B^2$ is of the order of 1 or less, relative errors in $M(x,t)$ and $C_f(x,t)/C_0$ will occur when values of C_f/C_0 are significantly greater than zero. Therefore, when θ_m^* is large, the criteria given by Eqs. (24a) and (24b) should be applicable for any value of t . When $D_e \theta_m^*/B^2$ is of the order of 1 or less, the criteria are also applicable, but the errors in radionuclide discharges calculated using the approximation will increase substantially as $D_e t^*/B^2$ becomes less than about 0.2.

Equivalent Porous Medium. In this approximation, it is assumed that relaxation times, denoted by t_r , for perturbations in radionuclide concentrations in the porous matrix are small relative to the time scale of interest. This assumption implies that the fracture fluid and porous matrix are in local equilibrium with respect to radionuclide diffusion. In which case, $\bar{H}(t)$ in Eq. (6) approaches unity during a time interval which is less than the time required for

$C_f(x,t)$ to change appreciably, and $M(x,t) = \phi_m^R C_f(x,t)$, which is obtained by integrating by parts in Eq. (6) and noting that $C_f(x,0) = 0 = \bar{H}(0)$ for $x > 0$. Eqs. (1) and (2) reduce to a single equation involving only C_f

$$\frac{\partial C_f}{\partial t} + \frac{v}{R_f} \frac{\partial C_f}{\partial x} = 0 \quad (25)$$

which has the solution

$$C_f(x,t) = C_0 S\left(t - \frac{R_f x}{v}\right) \quad (26)$$

where $S(t)$ denotes the Heaviside unit step function.

The validity of the equivalent-porous-medium approximation depends on the relaxation time t_r and the mean radionuclide residence time. Define t^* and θ_m^* as above. Again, assume that the mean radionuclide residence time is approximately the maximum residence time θ_m . If $t_r \ll \theta_m^*$, then perturbations in radionuclide concentrations would be exposed to fracture fluid and porous matrix near equilibrium. For purposes here, take t_r as the time required for $\bar{H}(t^*)$ to become approximately unity. From Table II, $t_r = 2B^2/D_e$, and a criterion for applying the equivalent-porous-medium approximation is $\theta_m^* = (x/v)(R_f - 1) \gg t_r = 2B^2/D_e$. Allowing for perturbations in concentration and heterogeneity in the system, a reasonable criterion would be⁹

$$\bar{\alpha} = \frac{D_m \phi_m R_f x}{v B^2} = \frac{D_m^2 \phi_m^2 x}{v B^2} \geq 50 \quad (27)$$

Provided that the above criterion is satisfied, the mean radionuclide residence time does correspond to the maximum residence time θ_m since the porous matrix and fracture fluid essentially are near equilibrium. The actual errors in $C_f(x,t)$ which result from applying the equivalent-porous-medium approximation are discussed below.

EVALUATION OF CRITERIA AND APPROXIMATIONS

To evaluate the above approximations, dimensionless breakthrough curves, C_f/C_0 versus \bar{Y}/\bar{X} were calculated using each of the three approximations. The approximate curves were then compared with the exact solution given by Eq. (3). The infinite integral in Eq. (3) was evaluated numerically using the method discussed by Rasmuson and Neretnieks.⁸ Results for $\bar{\alpha} = 0.2, 1.0,$ and 50 are shown on Figs. 4 through 6, respectively. For convenience in discussing these results, note that $(t - x/v)/(B^2/D_e) = \bar{Y}/\bar{X}$ and $(\theta_m - x/v)/(B^2/D_e) = \bar{\alpha}$; therefore $\bar{Y}/\bar{X} = 2(t - x/v)/(\theta_m - x/v) = 2t^*/\theta_m^*$.

First consider the semi-infinite-medium approximation. Fig. 4 shows that for $\bar{\alpha} = 0.2$, the approximation provides an excellent estimate for the exact solution when \bar{Y}/\bar{X} is less than 3, and at larger values of \bar{Y}/\bar{X} the relative errors in C_f/C_0 due to the approximation are small. Therefore, the more restrictive criterion given by Eq. (14a) appears valid, and as previously predicted, the errors resulting from using the approximation are not significant until

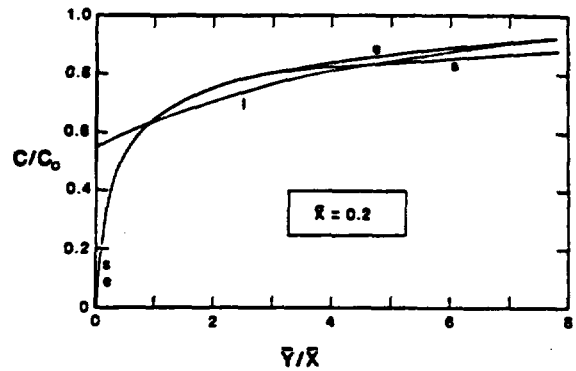


Fig. 4. Comparison of radionuclide discharges calculated from approximate and exact solutions when $\bar{\alpha} = 0.2$ (e, l, and s denote results for exact solution, linear-driving-force approximation, and semi-finite-medium approximation, respectively).

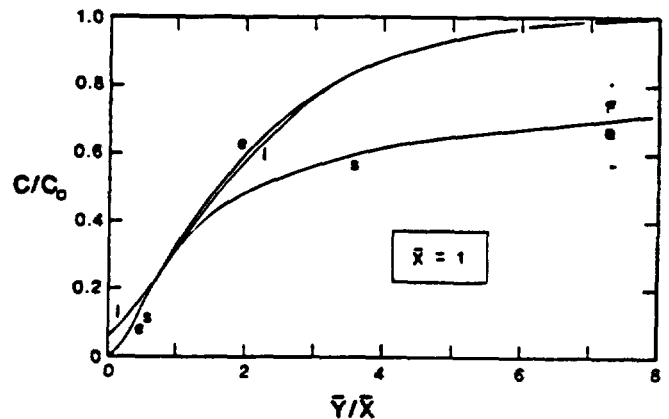


Fig. 5. Comparison of radionuclide discharges calculated from approximate and exact solutions when $\bar{\alpha} = 1.0$ (e, l, and s denote results for exact solution, linear-driving-force approximation, and semi-finite-medium approximation, respectively).

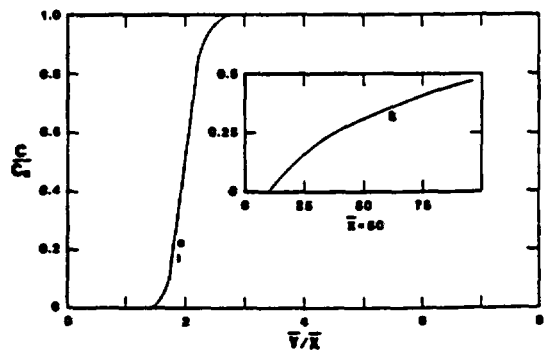


Fig. 6. Comparison of radionuclide discharges calculated from approximate and exact solutions when $\bar{\alpha} = 50$ (e, l, and s denote results for exact solution, linear-driving-force approximation, and semi-finite-medium approximation, respectively).

$t > \theta_m$ ($t = \theta_m$ when $\bar{V}/\bar{X} = 2$). Fig. 5 shows that for $\bar{X} = 1.0$, the approximation provides an excellent estimate for the exact solution when $\bar{V}/\bar{X} < 1$. As \bar{V}/\bar{X} approaches 2 (or $t/\theta_m = 1$), the relative error between approximate and exact solutions is about 20 to 30 percent, which is consistent with the errors previously predicted. Furthermore, the relative error does not increase appreciably as \bar{V}/\bar{X} (or t/θ_m) becomes large. Therefore, the less restrictive criterion given by Eq. (14b) appears valid, provided that the resulting errors in M and C_f/C_0 are acceptable. For $\bar{V}/\bar{X} > 1$, C_f/C_0 is underestimated because M is overestimated. Fig. 6 ($\bar{X} = 50$) shows that as \bar{X} becomes large, the semi-infinite-medium approximation becomes unacceptable.

Next, consider the linear driving force approximation. Figure 4 shows that for $\bar{X} = 0.2$, the approximation provides a reasonable estimate for the exact solution when \bar{V}/\bar{X} is about 0.4 or greater, and the less restrictive criterion given by Eq. (15b) appears valid, provided that $\bar{V}/\bar{X} > 0.4$ (or $t^*/(B^2/D_0) > 0.08$). Figure 5 shows that when $\bar{X} = 1$, the linear-driving-force approximation provides a very good estimate for the exact solution when \bar{V}/\bar{X} is again about 0.4 or greater. At lesser values of \bar{V}/\bar{X} , the relative error between approximate and exact solutions increases substantially, but the actual concentrations C_f/C_0 from either solution are small. Therefore, the more restrictive criterion given by Eq. (15a) should be generally applicable provided that small concentrations at early times need not be estimated accurately. On Fig. 6 ($\bar{X} = 50$), the curves for the linear-driving-force approximation and exact solution essentially coincide, which shows that the approximation provides an excellent estimate for the exact solution at large values of \bar{X} .

Also, from Figs. 5 and 6, it can be seen that at large \bar{X} , the mean radionuclide residence time is essentially θ_m .¹ As \bar{X} becomes small, the deviation in residence times about the mean increases, but the mean residence time remains on the order of θ_m .

Finally, consider the equivalent-porous-medium approximation. In Figs. 4-6, the approximate solution given by Eq. (26) corresponds to a vertical line at $\bar{V}/\bar{X} = 2$ (or $t = \theta_m$). The errors associated with equivalent-porous-medium approximations have been discussed previously.⁹ The essential features of those errors can be seen on Figs. 4-6. In particular, as breakthrough occurs (C_f/C_0 becomes nonzero), the exact solution appears to be "dispersed" about the solution for the equivalent porous medium. As \bar{X} becomes large, that apparent dispersion becomes smaller, and at sufficiently large \bar{X} and \bar{V}/\bar{X} , would have negligible effect on cumulative radionuclide discharges. For example, when $\bar{X} = 50$, the error in cumulative radionuclide discharges calculated using the equivalent-porous-medium approximation will be small provided that \bar{V}/\bar{X} is about 2.6 or greater. Therefore, the criterion given by Eq. (27) appears valid provided that the time period of interest corresponds to \bar{V}/\bar{X} less than about 1.4 or greater than about 2.6.

APPLICATIONS

Approximate methods for calculating radionuclide transport can be very useful in performance assessment studies. The approximations described above can easily be incorporated into transport codes and used to obtain realistic estimates of radionuclide releases.

The NWFT/DVM computer code¹⁰ was developed at Sandia National Laboratories to simulate contaminant

transport for performance assessment studies. The program represents a known velocity field as a simplified network of one-dimensional transport segments. It can model the transport of radionuclide decay chains of any length, with isotopes having different retardation factors, and with various types of source terms. A new version of NWFT/DVM¹¹ treats flow and transport through fractured, porous media. Advection is assumed to take place in a set of parallel fractures and radionuclides diffuse into the adjoining rock matrix. Both the linear-driving-force and the equivalent-porous-media approximations are available in this version of the code. The analytical solutions derived in the previous sections were used to benchmark the linear-driving-force approximation of this computer code.

Dimensionless breakthrough curves were calculated with NWFT/DVM for several values of \bar{X} using the linear-driving-force approximation. Parameter values used in the calculations are listed in Table III. Two sets of calculations were carried out to determine the effect of flow velocity on the breakthrough curves generated. In order to simulate breakthrough for different values of \bar{X} , discharges were calculated for several values of path length x . Representative results are compared to the exact analytical solution Eq. (3) and the analytical solution for the linear-driving-force assumption Eq. (16). The numerical solution of NWFT/DVM agrees well with the analytical solutions for both the high and low velocity cases for $\bar{X} = 1$ and $\bar{X} = 50$ (Figs. 7-9). In addition, the numerical linear-driving-force approximation of NWFT/DVM agrees well with the exact analytical solution for $\bar{X} = 0.2$ when $\bar{V}/\bar{X} > 2$.

Table III

Parameter Values for NWFT/DVM Calculations

Fracture Aperture $2b$	100 μm
Fracture Spacing $2(B+b)$	Case 1: 10 cm
	Case 2: 50 cm
Fracture Porosity ϕ_f	Case 1: 10^{-3}
	Case 2: 2×10^{-4}
Matrix Porosity ϕ_m	0.01
Tortuosity α^2	10
Molecular Diffusion Coefficient D	1.6×10^{-5} cm^2/s
Matrix Retardation Factor R_m	1.0
Fluid Velocity v	Case 1: 10 cm/day
	Case 2: 0.75 cm/day

Eqs. (24a), (24b), and (27) were used to identify geochemical and hydrological conditions under which the semi-infinite-medium, linear-driving-force, and equivalent-porous-medium approximations are valid. Fig. 10 illustrates the application of these criteria to site-specific data for tuff^{12,13} and basalt^{14,15} and generic data for granite.^{16,17,18} The plotted points bracket ranges of hydrological and geochemical parameters that are representative of these media. The parameter values used in constructing the plots have been tabulated by Erickson and others.¹⁹ Lines representing \bar{X} values of 0.2, 1, and 50 divide the graph into regions within which at least one of the approximations will provide acceptable results. It can be seen that for tuff, the equivalent-porous-medium approximation should usually be valid even for relatively thin beds ($x = 30$ m). For basalt and granite, the semi-infinite-medium approximation or

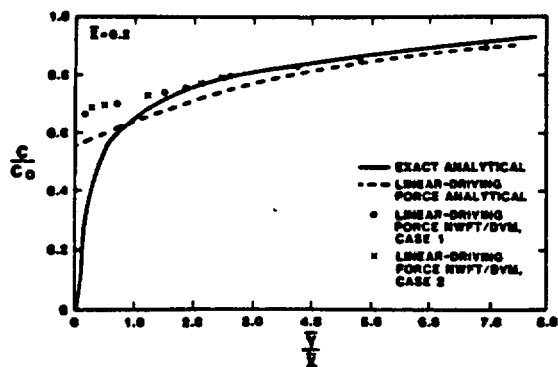


Fig. 7. Comparison of radionuclide discharges calculated with analytical exact solution and linear-driving-force approximation when $\bar{X} = 0.2$. For case 1, the fluid velocity = 10 cm/day and the distance from the source, x , is 36 cm. For case 2, fluid velocity = 0.75 cm/day and $x = 14$ cm. (See Table III.)

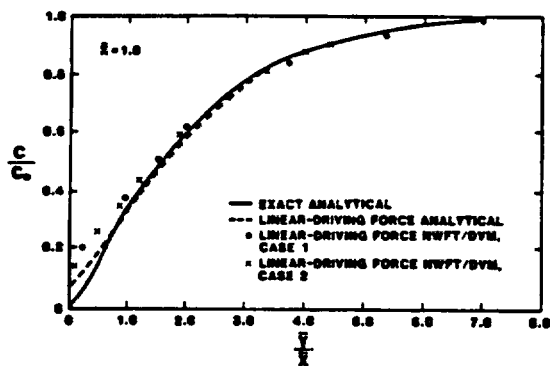


Fig. 8. Comparison of radionuclide discharges calculated with analytical exact solution and linear-driving-force approximation for $\bar{X} = 1.0$. For case 1, $x = 180$ cm; for case 2, $x = 68$ cm. See Table III for other parameter values.

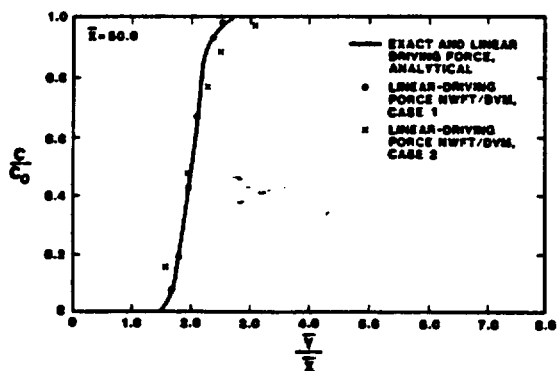


Fig. 9. Comparison of radionuclide discharges calculated with analytical exact solution and linear-driving-force approximation for $\bar{X} = 50$. For case 1, $x = 90.5$ m; for case 2, $x = 34$ m. See Table III for other parameter values.

the linear-driving-force approximation may be required for most calculations.

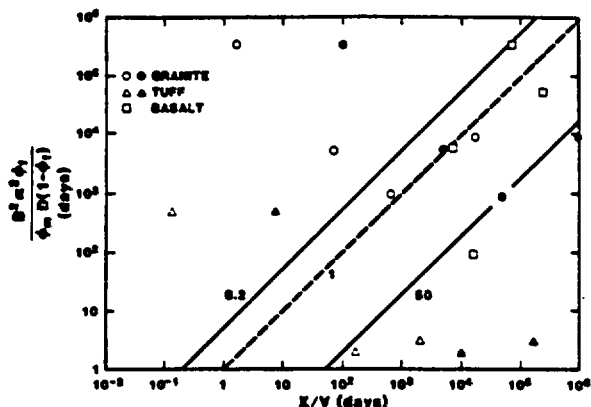


Fig. 10. Application of criteria to representative site-specific data for granite, basalt, and tuff. Numbers on lines are values of \bar{X} . Areas below lines marked '0.2' and '50' correspond to conditions under which linear-driving-force and porous-medium approximations, respectively, apply. The semi-infinite-medium approach applies in the area above the line marked '1'. Solid and open symbols refer to transport distances of $x = 2000$ m and $x = 30$ m, respectively.

CONCLUSIONS AND RECOMMENDATIONS

The results above are encouraging and indicate that the semi-infinite-medium, linear-driving-force, and equivalent-porous-medium approximations could be useful for performance assessment of HLW repositories in fractured, porous rock. The radionuclide discharges calculated by the linear-driving-force approximation used in the finite-difference code NWFT/DVM agree well with those calculated using an exact analytical solution for a range of hydrological parameters. Furthermore, the equivalent-porous-medium approximation could extend the results from Sandia's Geochemical Sensitivity Analysis Program to systems involving fractured, porous rock. However, additional evaluation is necessary. Cases must be examined in which the radionuclide material balances include terms for chemical reactions, radioactive decay, and production of nuclides. In addition, an assessment should be made of the sensitivity of the approximations to heterogeneities in fracture spacing, aperture and geometry and the presence of fracture-fill minerals.

ACKNOWLEDGMENT

The authors wish to thank Robert Guzowski for compiling data on the properties of basaltic rock used in Fig. 10. They would also like to thank Rob Rechar and William Casey for reviewing the manuscript. This work was supported by the United States Nuclear Regulatory Commission and performed at Sandia National Laboratories which is operated for the U.S. Department of Energy under Contract Number DE-AC04-76DP00789.

REFERENCES

1. J. B. ROSEN, "Kinetics of a Fixed Bed System for Solid Diffusion into Spherical Particles," J. Chemical Physics, 20, 387 (1952).
2. H. S. CARSLAW and J. C. JAEGER, Conduction of Heat in Solids, 2nd ed., p. 483, Clarendon Press, Oxford (1959).
3. K. L. ERICKSON and D. R. FORTNEY, Preliminary Transport Analyses for Design of the Tuff Radionuclide Migration Field Experiment, p. 12, SAND81-1253, Sandia National Laboratories, Albuquerque, New Mexico (1981).
4. J. CRANK, The Mathematics of Diffusion, p. 32, Clarendon Press, Oxford (1975).
5. Ibid., p. 48.
- R. COURANT, Differential and Integral Calculus, Vol. 2, 2nd ed., p. 128, Interscience Publishers (1937).
7. T. K. SHERWOOD, R. L. PIGFORD, and C. R. WILKE, Mass Transfer, pp. 554-571, McGraw-Hill, New York (1975).
8. A. RASMUSON and I. NERETNIEKS, "Migration of Radionuclides in Fissured Rock: The Influence of Micropore Diffusion and Longitudinal Dispersion," J. Geophys. Res., 86, p. 3749 (1981).
9. K. L. ERICKSON, "Approximations for Adapting Porous Media Radionuclide Transport Models to Analysis of Transport in Jointed, Porous Rock," Materials Research Society Symposium Proceedings, Vol. 15, pp. 473-480, Elsevier, New York (1983).
10. J. E. CAMPBELL, D. E. LONGSINE, and R. M. CRANWELL, "Risk Methodology for Geologic Disposal of Radioactive Waste: The NWFT/DVM Computer Code User's Manual," NUREG/CR-2081, Sandia National Laboratories, Albuquerque, New Mexico (1981).
11. E. J. BONANO, M. S. Y. CHU, R. M. CRANWELL, and P. A. DAVIS, "Development of a Performance Assessment Methodology for Nuclear Waste Isolation in Geologic Media," SAND85-0456C, Sandia National Laboratories, Albuquerque, New Mexico (1985).
12. M. D. SIEGEL, M. S. Y. CHU, and R. E. PEPPING, "A Simplified Analysis of a Hypothetical Repository in a Tuff Formation," Technical Assistance for Regulatory Development: Review and Evaluation of the Draft EPA Standard 40CFR191 for Disposal of High-Level Waste, Vol. 3, NUREG/CR-3235, Sandia National Laboratories, Albuquerque, New Mexico (1983).
13. P. TIEN, M. D. SIEGEL, C. D. UPDEGRAFF, K. K. WAHI, and R. V. GUZOWSKI, "Repository Site Data for Unsaturated Tuff, Yucca Mountain, Nevada," NUREG/CR-4110, Sandia National Laboratories, Albuquerque, New Mexico (1985).
14. W. W. LOO, R. C. ARNETT, L. S. LEONHART, S. P. LUTTRELL, S. P. WANG, and W. R. McSPADDEN, "Effective Porosities of Basalt: A Technical Basis for Values and Probability Distributions Used in Preliminary Performance Assessments," RHO-SD-BWI-TI-254, Rockwell Hanford Operations, Richland, Washington (1985).
15. P. E. LONG, "Repository Horizon Identification, Draft," Vol. 1, RHO-SD-BWI-TY-001, Rockwell Hanford Operations, Richland, Washington (1983).
16. I. NERETNIEKS, "Diffusion in the Rock Matrix: An Important Factor in Radionuclide Retardation?," J. Geophys. Res., 85, 4379 (1980).
17. L. BIRGERSSON and I. NERETNIEKS, "Diffusion in the Matrix of Granitic Rock, Field Test in the Stripa Mine," Scientific Basis for Nuclear Waste Management, Vol. 7, p. 247, North Holland, New York (1984).
18. L. CARLSSON, A. WINBERG, and B. ROSANDER, "Investigations of Hydraulic Properties in Crystalline Rock," Scientific Basis for Nuclear Waste Management, Vol. 7, p. 255, North Holland, New York (1984).
19. K. L. ERICKSON, M. D. SIEGEL, and M. S. Y. CHU, "Approximate Methods for Analyzing Radionuclide Transport in Fractured Porous Rock," SAND85-1645, Sandia National Laboratories, Albuquerque, New Mexico (in preparation).